Synthesis and Structural Characterization of Metallacarboranes Containing Bridged Dicarbollide Ligands

Frank A. Gomez,† Stephen E. Johnson,‡ Carolyn B. Knobler, and M. Frederick Hawthorne*

Department of Chemistry and Biochemistry, University of California,
Los Angeles, California 90024-1569

Received February 2, 1992

The synthesis and characterization of a family of carbon-bridged metallacarboranes of the type [7,7′-μ-1,*n*-C_nH_{2n}-(7,8-$C_2B_9H_{10})_2$M]$^-$ (*n* = 3, M = Co^{3+} (**14**); *n* = 4, M = Co^{3+} (**15**), Fe^{3+} (**16**), Ni^{3+} (**17a**), Cr^{3+} (**18**); *n* = 5, M = Co^{3+} (**19**)) and [7,7′-μ-1,5-TosN(CH_2CH_2–)$_2$-(7,8-$C_2B_9H_{10})_2$M]$^-$ (M = Co^{3+} (**20**), Fe^{3+} (**21**)) are described. In each instance, meso and *dl* isomers were obtained from the reaction of the diastereomeric bridged carborane precursors and metal halide. The tosylated derivatives were separated into meso and *dl* isomers by HPLC techniques, and all diastereomeric metallacarboranes were spectroscopically characterized. Compounds **14–16** and **17b** (Ni^{4+}) have been structurally characterized by single-crystal X-ray diffraction. Compound **14** crystallizes in the triclinic space group $P\bar{1}$ with *a* = 10.056 (8) Å, *b* = 11.861 (9) Å, *c* = 17.896 (11) Å, α = 96.20 (2)°, β = 96.36 (3)°, γ = 111.20 (3)°, *V* = 1952 Å^3, *Z* = 2, and *R* = 0.089. Compound **15** crystallizes in the triclinic space group $P\bar{1}$ with *a* = 9.979 (8) Å, *b* = 11.769 (1) Å, *c* = 17.640 (1) Å, α = 84.46 (2)°, β = 83.61 (2)°, γ = 112.79 (2)°, *V* = 1876 Å^3, *Z* = 2, and *R* = 0.054. Compound **16** crystallizes in the orthorhombic space group *B2cb* (standing setting *Aba*2) with *a* = 9.616 (4) Å, *b* = 10.768 (4) Å, *c* = 18.326 (7) Å, *V* = 1897 Å^3, *Z* = 4, and *R* = 0.027. Compound **17b** crystallizes in the monoclinic space group *C*2/*c* with *a* = 21.726 (5) Å, *b* = 9.906 (2) Å, *c* = 35.767 (9) Å, β = 103.04 (9)°, *V* = 7499 Å^3, *Z* = 8, and *R* = 0.090. The relationship between bridge length and complex formation is examined.

Introduction

Since the initial report[1] of the preparation of the first metallacarborane, [3,3′-Fe^{II}(1,2-$C_2B_9H_{11})_2$]$^{2-}$, metallacarborane chemistry has expanded in both scope and diversity and has provided a host of potentially useful applications. Only recently has possible use of metallacarboranes as radiometal carriers for radioimmunodiagnosis and radioimmunotherapy been suggested. We have now developed a series of extraordinarily stable metallacarborane derivatives which employ a pyrazole moiety bridging two dicarbollyl fragments via boron–nitrogen (B–N) bonds. The properties of these novel species, Venus flytrap clusters (VFC), suggested the use of functionalized VFC systems for binding radiotransition metals to tumor-associated monoclonal antibodies, thus providing conjugates that are clinically useful for radioimmunodiagnosis and radioimmunotherapy.[2]

The first reported bridged metallacarborane[3] contained a zwitterionic –S–C^+H–S– array which linked B-atoms of separate dicarbollide ligands. In later work, bridged metallacarboranes have been reported[4] which were B–E (O, Se, Te, N, S = E) linked[4] to the participating dicarbollyl moieties. More recently, a 1,2-phenylene-bridged cobaltacarborane was synthesized from an arenediazonium salt.[5] In all cases except one,[5b] the metal complex [3,3′-Co^{III}(1,2-$C_2B_9H_{11})_2$]$^{2-}$ served as the starting material and the bridged species were typified by boron–sulfur (B–E) or boron–carbon (B–C) cage linkages. To date no carbon–carbon (C–C) cage-linked metallacarboranes have been reported, although use of the *tert*-butyldimethylsilyl protecting group has, for the first time, made possible the facile synthesis of C–C-linked carboranes and their corresponding dicarbollide ligands.[6] In this same vein, we assumed that there must exist an optimal bridge length between dicarbollide moieties which would facilitate metal ion insertion. To test this hypothesis, a series of cage-carbon-linked alkylene-bridged carboranes and an azaalkylene-bridged carborane were constructed and converted to bridged *commo*-bis(dicarbollide) derivatives of a variety of transition metals. The design and synthesis of models of these second generation VFC reagents are described herein.

Results and Discussion

These second-generation Venus flytrap cluster (VFC) species represent further efforts toward the rational design of catabolism resistant inorganic imaging agents and radiopharmaceuticals.[2] The alkylene-bridged, cage-carbon-linked compounds presented here differ from formerly reported bridged derivatives. Previously known bridged metallacarboranes, with the single exception of the pyrazole-bridged (VFC) species,[2] were synthesized by attachment of the bridge to the preformed metallacarboranes.[3-5] In the present case, dicarbollide ligands are linked together prior to metal complexation. Formation of the required prelinked dicarbollide ligand systems was possible through the use of *tert*-butyldimethylsilyl protected carborane.[6] These compounds are the first examples of carbon-bridged and carbon-linked metallacarboranes. In all previously reported bridged metallacarboranes the bridge is linked through boron atoms of the carborane

† National Institutes of Health Minority Access to Research Careers Predoctoral Fellow (1986–1991).

‡ National Science Foundation Postdoctoral Fellow (1990–1992).

(1) (a) Young, D. C.; Wegner, P. A.; Hawthorne, M. F. *J. Am. Chem. Soc.* **1965**, *87*, 1818. (b) Andrews, T. D.; Hawthorne, M. F. *J. Chem. Soc., Chem. Commun.* **1965**, 19. (c) Hawthorne, M. F. *Boron Hydride Chemistry*; Muetterties, E. L., Ed.; Academic Press, Inc.: New York, 1975; p 383. (d) Hawthorne, M. F.; Young, D. C.; Andrews, T. D.; Howe, D. V.; Pilling, R. L.; Pitts, A. D.; Reintjes, M.; Warren, L. F.; Wegner, P. A. *J. Am. Chem. Soc.* **1968**, *90*, 879.

(2) (a) Hawthorne, M. F.; Varadarajan, A.; Knobler, C. B.; Chakrabarti, S.; Paxton, R. J.; Beatty, B. G.; Curtis, F. L. *J. Am. Chem. Soc.* **1990**, *112*, 5365. (b) Paxton, R. J.; Beatty, B. G.; Hawthorne, M. F.; Varadarajan, A.; Williams, L. E.; Curtis, F. L.; Knobler, C. B.; Beatty, J. D.; Shively, J. E. *Proc. Natl. Acad. Sci.* **1991**, *88*, 3387.

(3) (a) Churchill, M. R.; Gold, K.; Francis, J. N.; Hawthorne, M. F. *J. Am. Chem. Soc.* **1969**, *91*, 1222. (b) Francis, J. N.; Hawthorne, M. F. *Inorg. Chem.* **1971**, *10*, 594.

(4) (a) Plesek, J.; Hermanek, S.; Base, K.; Todd, L. J.; Wright, W. F. *Collect. Czech. Chem. Commun.* **1976**, *41*, 3509. (b) Janousek, A.; Plesek, J.; Hermanek, S.; Base, K.; Todd, L. J.; Wright, W. F. *Collect. Czech. Chem. Commun.* **1981**, *46*, 2818.

(5) (a) Francis, J. N.; Jones, C. J.; Hawthorne, M. F. *J. Am. Chem. Soc.* **1972**, *94*, 4878. (b) Shelly, K.; Knobler, C. B.; Hawthorne, M. F. *New J. Chem.* **1988**, *12*, 317.

(6) (a) Gomez, F. A.; Johnson, S. E.; Hawthorne, M. F. *J. Am. Chem. Soc.* **1991**, *113*, 5915. (b) Gomez, F. A.; Hawthorne, M. F. *J. Org. Chem.* **1992**, *57*, 1384.

0020-1669/92/1331-3558$03.00/0

Scheme I

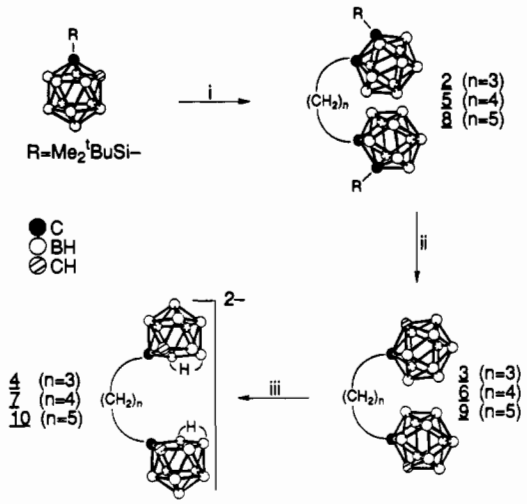

i. (a) nBuLi (b) $Br(CH_2)_nBr$, n=3-5; ii. $(nBu)_4NF$, –76° to 0°C. iii. (a) KOH/EtOH, (b) CsCl.

cage.[2-5,7] Consequently, the compounds described here represent a new class of alkylene carbon-bridged metallacarboranes.

Synthesis and Spectroscopic Characterization of Bridged Metallacarboranes. Alkylene-bridged bis(dicarbollide) ligands **4**, **7**, and **10** were synthesized in three steps (Scheme I). The reaction of 0.5 molar equiv of the appropriate alkyl dibromide ($Br(CH_2)_nBr$, where n = 3–5) and 1.0 molar equiv of 1-lithio-2-*tert*-butyldimethylsilyl-1,2-dicarba-*closo*-dodecaborane (12) (**1**)[6] in 2:1 C_6H_6/Et_2O results in the formation of the disilylated bridged species **2**, **5**, and **8** in 61%, 70%, and 53% yield, where n = 3, 4, and 5, respectively. Deprotection of **2**, **5**, and **8** with tetrabutylammonium fluoride (TBAF)[8] in THF (–76 to 0 °C) afforded the corresponding desilylated species **3** (88%), **6** (92%), and **9** (88%), respectively. Subsequent base degradation[9] with potassium hydroxide in ethanol yielded the corresponding dianion species **4** (61%), **7** (80%), and **10** (54%) as their cesium salts. These salts are very soluble in tetrahydrofuran and thermally stable, and they may be handled for prolonged periods of time in the air.

Species **4**, **7**, and **10** were characterized by a combination of ^1H, ^{11}B, and ^{13}C NMR, IR, and mass spectroscopy. The ^1H NMR spectrum of these compounds in acetone-d_6 displays a single carboranyl C–H resonance and alkylene-related multiplets in addition to broad, complex B–H resonances characteristic of the dicarbollide cage. The ^{11}B NMR spectrum exhibits resonances with an area ratio of 2:1:3:1:1:1 consistent with 7,8-dicarbollide cages. The IR spectra contain a characteristic band at 2523 cm^{-1} assigned to the B–H stretching mode, while the mass spectra exhibit strong parent ion envelopes.

Treatment of the trimethylene-bridged species **4** with excess NaH in tetrahydrofuran afforded the desired bridged dicarbollide anion,[10] which was subsequently added to a suspension of anhydrous cobalt chloride in THF (Scheme II). Cobaltacarborane **14** was isolated as its triphenylmethylphosphonium salt in 46% yield. Separation of the *dl* and meso isomers by column chromatography or by HPLC techniques was not successful. The ^{11}B NMR spectrum of **14** exhibited a group of peaks consistent with a set of isomers.

Scheme II

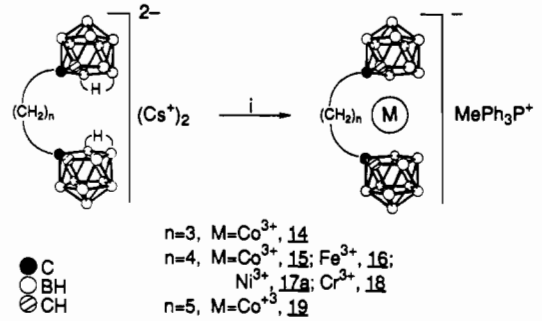

i. (a) NaH/THF (b) metal halide, THF (c) PPh_3MeBr.

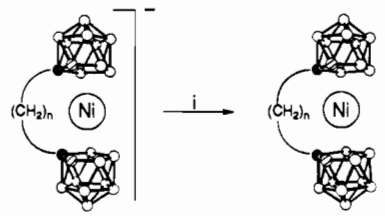

i. $FeCl_3$, CH_3CN/H_2O **17b**

The tetramethylene-bridged species **7** proved to be a more efficient ligand for metallacarborane formation. Under conditions similar to those employed for the synthesis of **14**, the cobaltacarborane **15** was obtained in 61% yield. The paramagnetic iron, **16**, and chromium, **18**, derivatives were similarly obtained in 41% and 39% yields, respectively (Scheme II). No ^{11}B-^1H spin-couplings were observed[11] in their ^{11}B NMR spectra, which extended over approximately 650 ppm. The wide separation of the individual ^{11}B resonances is due to the presence of large paramagnetic contact shifts[1d] which involve the paramagnetic iron(III) atom. The broad upfield resonances in **16** arise from the three boron atoms nearest iron(III) in **16**.[1d,12] A similar ^{11}B NMR pattern is observed for **18**, although the magnitude of the paramagnetic contact shift is not as large.

The nickelacarborane, **17a**, which contains formal nickel(III) was prepared under similar conditions as a green solid. This compound exhibited broad ^{11}B NMR resonances between 160 and –200 ppm, characteristic of large paramagnetic contact and pseudocontact shifts.[13] Subsequent oxidation with $FeCl_3$ afforded the formal nickel(IV) complex (**17b**) in 58% yield from **7** (Scheme II). The resulting nickelacarborane was diamagnetic and exhibited resonances consistent with a set of isomers. The pentamethylene-bridged cobaltacarborane **19** was obtained under similar reaction conditions in 20% yield from **10**.

The azaalkylene-bridged ligand **13** was synthesized in four steps (Scheme III). The reaction of 0.6 molar equiv of diethanolamine tritosylate[14] and 1.0 molar equiv of 1-lithio-2-*tert*-butyldimethylsilyl-1,2-dicarba-*closo*-dodecaborane(12) (**1**)[6] in 2:1 C_6H_6/Et_2O results in the formation of the bridged species **11**. Subsequent deprotection with TBAF (**12**; 99% yield) and base degradation (47% yield) afforded **13** as its cesium salt.

Compound **13** was characterized by a combination of ^1H, ^{11}B, and ^{13}C NMR, IR, and mass spectroscopy. The ^1H NMR spectrum exhibits two doublets for the tolyl moiety and multiplets for the dimethylene fragments. A single carboranyl C–H resonance and complex B–H resonances are observed. The ^{11}B NMR spectrum exhibits resonances with an area ratio of 2:1:

(7) Varadarajan, A.; Johnson, S. E.; Chakrabarti, S.; Gomez, F. A.; Knobler, C. B.; Hawthorne, M. F. Submitted for publication.
(8) Corey, E. J.; Venkateswarlu, A. *J. Am. Chem. Soc.* **1972**, *94*, 6190.
(9) (a) Wiesboeck, R. A.; Hawthorne, M. F. *J. Am. Chem. Soc.* **1964**, *86*, 1642. (b) Hawthorne, M. F.; Young, D. C.; Garrett, P. M.; Owen, D. A.; Schwerin, S. G.; Tebbe, F. N.; Wegner, P. A. *J. Am. Chem. Soc.* **1968**, *90*, 862.
(10) Deprotonation using *n*-BuLi in hexane resulted in significantly lowered yields of bridged metallacarborane product: Gomez, F. A. Ph.D. Dissertation, UCLA, 1991.
(11) Lipscomb, W. N.; Kaczmarczyk, A. *Proc. Natl. Acad. Sci. USA* **1961**, *47*, 1796.
(12) (a) Pilling, R. L.; Hawthorne, M. F. *J. Am. Chem. Soc.* **1965**, *87*, 3987. (b) Wiersema, R. J.; Hawthorne, M. F. *J. Am. Chem. Soc.* **1974**, *96*, 761.
(13) Warren, L. F.; Hawthorne, J. F. *J. Am. Chem. Soc.* **1970**, *92*, 1157.
(14) Searle, G. H.; Geue, R. J. *Aust. J. Chem.* **1984**, *37*, 959.

Scheme III

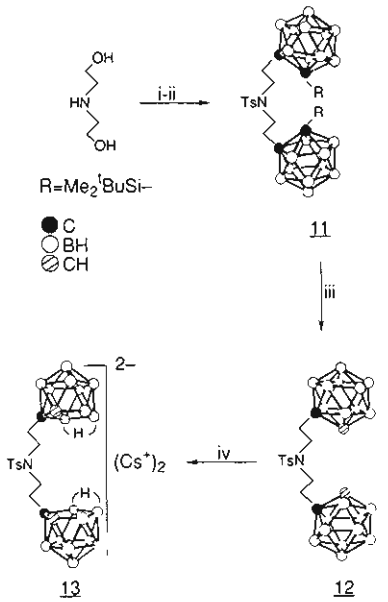

i. TsCl, pyridine; ii. (a) 1 (b) nBuLi, C_6H_6/ET_2O; iii. Bu_4NF, THF, −76° to 0°C.; iv. (a) KOH, EtOH (b) CsCl

Scheme IV

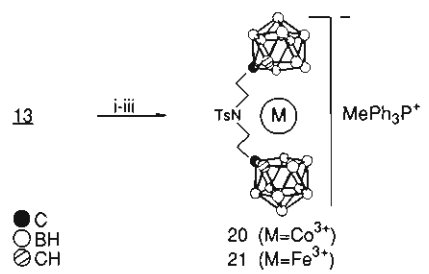

i. NaH/THF; ii. $CoCl_2$ or $FeCl_2$; iii. PPh_3MeBr

1:2:1:1:1. The IR contains a band at 2512 cm^{-1} assigned to the B–H stretching mode, and the mass spectrum exhibits a strong anion envelope.

Using **13** as a starting material, the cobalta-, **20**, and ferracarboranes, **21**, were obtained as previously described in 61% and 59% yield, respectively (Scheme IV). The ^{11}B NMR spectra of **20** and **21** exhibited resonances consistent with a mixture of isomers, *dl* and meso, and the respective meso and *dl* isomers of **20** and **21** were separated by HPLC techniques. Ferracarborane **20** is paramagnetic and exhibits ^{11}B NMR resonances consistent with those observed with other paramagnetic species.[1d,12] The boron atoms on the face, closest to the iron atom, were observed as broad resonances near −525 ppm.[12b]

A comparison of yields between cobaltacarboranes gives the following sequence: **15** > **20** > **14** > **19**. This suggests that the four-carbon bridge present in the precursor **7** provides a more favorable system than the others. It appears that **4**, with a trimethylene bridge, provides too short a chain to allow necessary flexibility as demonstrated in the lower yield of **14**. On the other hand, the pentamethylene bridge in **10** is apparently too long, and this chain length is entropically unfavorable. The higher yield of **15** suggests that **7** provides the proper balance of dynamic and entropy factors.

The synthesis of **20** is noteworthy, since it is a five-atom-bridged derivative similar to **19**. In fact, **20** was formed in a higher yield than were **14** and **19**. It is not unreasonable to expect that the interaction of the lone pair of electrons on the bridge nitrogen of the ligand and a transition metal ion might provide a favorable chelation effect. A molecular model demonstrates that the tosyl group present in **13** forces the alkylene arms and their carborane ligands toward one another. Thus, **13** prefers to exist in a nonlinear conformation, which allows the dicarbollide moieties to approach one another, thereby facilitating the formation of **20** and **21**.

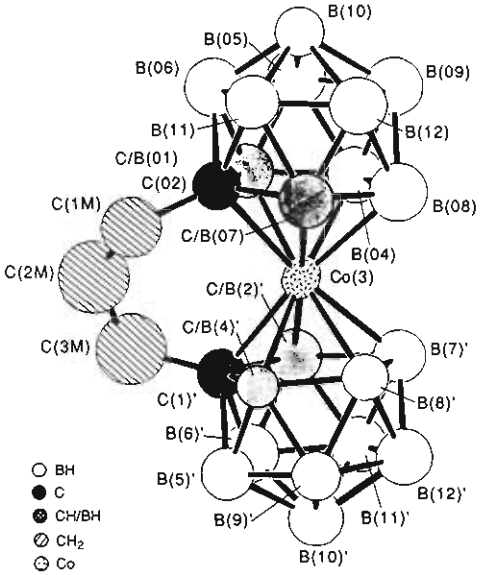

Figure 1. ORTEP representation of **14**, showing the numbering scheme. All hydrogen atoms were removed for clarity. Ellipsoids were drawn at the 0.50 probability level.

Table I. Selected Interatomic Distances and Angles for **14**

Distances (Å)			
Co(3)–C(02)	2.10 (7)	Co(3)–C/B(01)	2.09 (2)
Co(3)–B(04)	2.09 (3)	Co(3)–B(08)	2.19 (3)
Co(3)–C/B(07)	2.09 (2)	C(02)–C/B(01)	1.64 (3)
C(02)–B(11)	1.76 (3)	C(02)–C/B(07)	1.75 (3)
B(11)–B(06)	1.75 (4)	C(02)–C(1M)	1.57 (3)
C(1M)–C(2M)	1.45 (4)	C(2M)–C(3M)	1.52 (4)
Bond Angles (deg)			
C(02)–Co(3)–C(1′)	101.9 (8)	C(02)–C(1M)–C(2M)	116 (2)
Co(3)–C(02)–C(1M)	109.8 (3)	C(1M)–C(2M)–C(3M)	129 (2)

Description of the Molecular Structure of $14 \cdot {}^1/_2CH_2Cl_2$. The molecular structure of **14** is presented in Figure 1, and Table I lists selected interatomic distances and angles. The cobalt atom is bound in an η^5 fashion to the five-membered face of each of two dicarbollide ligands. The distance of the cobalt atom to each mean plane of the dicarbollide cage faces is 1.507 (3) and 1.491 (3) Å, comparable to other cobaltacarboranes.[15] Each of the bonding faces of the dicarbollide moieties is planar to within 0.01 (3) Å. The two faces are staggered rather than eclipsed. Consequently, the bonding face of each icosahedral moiety nearly eclipses the lower belt of the other icosahedral fragment. The structure of **14** may be compared to another bridged cobaltacarborane complex, $[HCS_2(C_2B_9H_{10})_2Co]$.[3] In this compound, the two dicarbollide ligands are connected to each other at the 10-position by a planar dithioformate bridge. The bridged cages must twist at the point of juncture with the bridging group in order to approach the required bonding distance to metal. The carborane faces are staggered, and the plane of the bridging HCS_2 group is not perpendicular to the plane of the C_2B_3 faces. The angle between normals to these two bonding planes in **14** is 7 (2)°. Planes through lower belt [B(02)–B(06)] atoms are nearly parallel to their respective metal-bonding (or upper belt) faces and atoms do not deviate by more than 0.03 (3) Å from their respective planes. Cobalt–carbon distances range from 2.07 (2) to 2.10 (2) Å (4 distances, average 2.09 Å), and cobalt–boron

(15) Zalkin, A.; Hopkins, T. E.; Templeton, D. H. *Inorg. Chem.* **1967**, *6*, 1911.

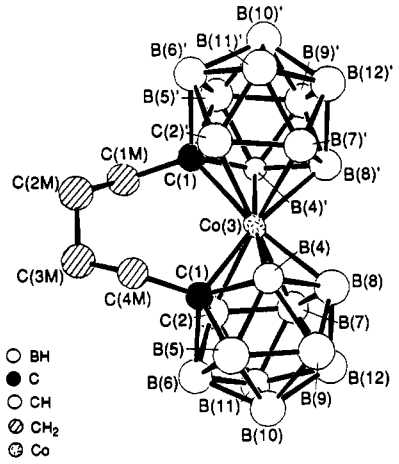

Figure 2. ORTEP representation of **15**, showing the numbering scheme. All hydrogen atoms were removed for clarity. Ellipsoids were drawn at the 0.50 probability level.

Table II. Selected Interatomic Distances and Angles for **15**

Distances (Å)			
Co(3)–C(1)	2.12 (2)	Co(3)–C(2)	2.10 (2)
Co(3)–B(7)	2.15 (3)	Co(3)–B(8)	2.13 (3)
Co(3)–B(4)	2.07 (3)	C(1)–C(2)	1.70 (3)
C(1)–B(5)	1.69 (3)	C(1)–B(4)	1.65 (3)
B(5)–B(6)	1.68 (4)	C(1)–C(4M)	1.56 (3)
C(4M)–C(3M)	1.52 (3)	C(3M)–C(2M)	1.55 (3)
C(2M)–C(1M)	1.54 (3)		

Bond Angles (deg)			
C(1)–Co(3)–C(1′)	108 (2)	C(1)–C(4M)–C(3M)	120.2 (16)
Co(3)–C(1)–C(4M)	115.9 (12)	C(4M)–C(3M)–C(2M)	116.7 (16)

distances range from 2.09 (2) to 2.19 (3) Å (6 distances, average 2.14 Å). These values are in good agreement with the mean Co–B (or C) distance of 2.07 Å in $Cs^+[(C_2B_9H_{11})_2Co]^-$.[15] All interatomic distances of the icosahedral cage are within the normal range found in *closo*-MC_2B_9 complexes.[16]

The complex **14** exhibited crystallographic disorder such that only the atom of the C_2B_3 bonding faces which was attached to the bridge could be assigned as carbon. The two adjacent atoms were treated as half-carbon, half-boron. Disorder of this type is fairly common for metallacarborane dicarbollide complexes[17] in which free rotation of the dicarbollide ligands is permitted. In the present case this observed disorder must arise from the cocrystallization of isomorphous diastereomers.

The two icosahedra which share the cobalt atom as a common apex in **14** are further linked via a $-(CH_2)_3-$ bridge which spans C(02) and C(1′).

Description of the Molecular Structure of 15. The molecular structure of **15** is presented in Figure 2, and Table II lists selected interatomic distances and angles. As in the case of **14**, the cobalt atom is bound in an η^5 fashion to the five-membered face of each of two dicarbollide moieties. The distance of the cobalt atom to each mean plane of the dicarbollide cage faces is 1.506 (3) and 1.524 (3) Å, which is comparable to **14** and other cobaltacarboranes.[15] Each of the bonding faces of the dicarbollide ligands is planar to within 0.03 (7) Å and staggered rather than eclipsed. As in the case of **14**, the bridged dicarbollide cages adjust themselves with respect to the bridge in order to achieve bonding with the metal. The result is that the carborane faces become staggered. The effect of the longer bridge length is shown in the increased angle between normals to these two bonding planes, 9 (2)° in **15** versus 7 (2)° in **14**. Planes through the lower belt [B(5)–B(6)–B(11)–B(12)–B(9)] atoms are nearly parallel to their respective metal-bonding (or upper belt) faces, and atoms in these planes do not deviate by more than 0.02 (3) Å from their respective planes. Cobalt–carbon distances range from 2.09 (2) to 2.12 (2) Å (average 2.10 Å), and cobalt–boron distances range from 2.07 (3) to 2.15 (3) Å (average 2.11 Å) in good agreement with other cobaltacarboranes.[15] All interatomic distances of the icosahedral cage are within the normal range found in *closo*-MC_2B_9 complexes.[16] The two icosahedra are bridged via a $-(CH_2)_4-$ chain which is linked to atoms C(1) and C(1)′.

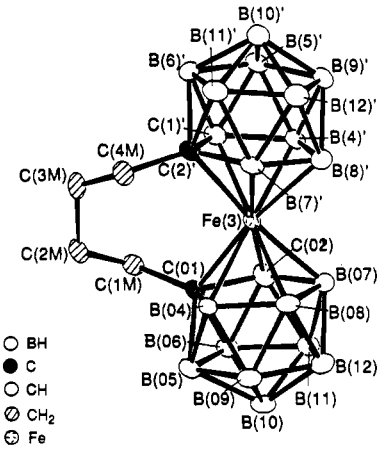

Figure 3. ORTEP representation of **16**, showing the numbering scheme. All hydrogen atoms were removed for clarity. Ellipsoids were drawn at the 0.50 probability level.

Table III. Selected Interatomic Distances and Angles for **16**

Distances (Å)			
Fe(3)–C(01)	2.138 (4)	Fe(3)–C(02)	2.096 (4)
Fe(3)–B(07)	2.120 (5)	Fe(3)–B(08)	2.146 (5)
Fe(3)–B(04)	2.124 (4)	C(01)–C(02)	1.650 (16)
C(01)–B(04)	1.659 (6)	C(01)–B(05)	1.729 (6)
B(05)–B(06)	1.751 (7)	C(01)–C(1M)	1.540 (6)
C(1M)–C(2M)	1.535 (6)	C(2M)–C(3M)	1.533 (6)
C(3M)–C(4M)	1.539 (6)		

Bond Angles (deg)			
C(01)–Fe(3)–C(2′)	108.5 (2)	C(01)–C(1M)–C(2M)	117.1 (3)
Fe(1)–C(01)–C(1M)	115.1 (3)	C(1M)–C(2M)–C(3M)	117.7 (4)

Description of the Molecular Structure of 16. The molecular structure of **16** is presented in Figure 3, and Table III lists selected interatomic distances and angles. The iron atom is bound in an η^5 fashion to the five-membered face of each of two dicarbollide faces. The distances of the iron atom to each mean plane of the dicarbollide cage faces are 1.545 (1) and 1.546 (1) Å, comparable to other ferracarboranes.[18] Each of the bonding faces of the dicarbollide moieties is planar to within 0.005 (5) Å, and these faces similarly are staggered rather than eclipsed. Consequently, the bonding face of each icosahedral moiety nearly eclipses the lower belt of the other icosahedral fragment. The bridged cages must rotate from the bridging group in order to approach the proper distance for bonding metal. The result is that the carborane faces become staggered. In **16** the angle between normals to these two bonding planes is 8.7 (3)° comparable to 9 (2)° in **15**. This is expected since iron(III) and cobalt(III) both have comparable ionic radii, 0.72 and 0.74 Å, respectively. Planes through lower belt [B(5)–B(6)–B(9)–B(11)–B(12)] atoms are nearly parallel to their respective bonding (or upper belt) faces, and atoms do not deviate by more than 0.005 (5) Å from these planes. Iron–carbon distances range from 2.096 (4) to 2.146 (5) Å (average 2.12 Å), and iron–boron distances range from 2.102

(16) Grimes, R. N. In *Comprehensive Organometallic Chemistry*; Wilkinson, G., Stone, F. G. A., Abel, E. W., Eds.; Pergamon: New York, 1982; Vol 1, Chapter 5 and references therein.

(17) For example, see: Hardy, G. E.; Callahan, K. P.; Strouse, C. E.; Hawthorne, M. F. *Acta Crystallogr., Sect. B* **1976**, *B32*, 264.

(18) Kang, H. C.; Lee, S. L.; Knobler, C. B.; Hawthorne, M. F. *Inorg. Chem.* **1991**, *30*, 2024.

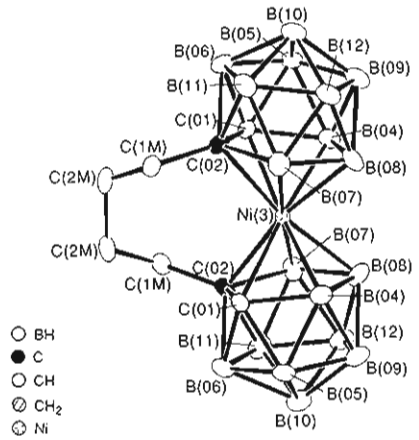

Figure 4. ORTEP representation of **17b**, showing the numbering scheme. All hydrogen atoms were removed for clarity. Ellipsoids were drawn at the 0.50 probability level.

Table IV. Selected Interatomic Distances and Angles for **17b**

Distances (Å)			
Ni(3)–C(02)	2.158 (5)	Ni(3)–C(01)	2.086 (5)
Ni(3)–B(04)	2.068 (16)	Ni(3)–B(08)	2.103 (6)
Ni(3)–B(07)	2.112 (4)	C(02)–C(01)	1.655 (7)
C(02)–B(07)	1.691 (9)	C(02)–B(06)	1.747 (7)
C(02)–B(11)	1.715 (7)	B(06)–B(11)	1.781 (9)
C(02)–C(1M)	1.519 (7)	C(1M)–C(2M)	1.524 (6)
C(2M)–C(2M)	1.5389 (6)		
Bond Angles (deg)			
C(02)–Ni(3)–C(01)/ C(02)	102.9 (2)	C(02)–C(1M)–C(2M)	120.3 (4)
		C(1M)–C(2M)–C(3M)	116.8 (3)
Ni(1)–C(02)–C(1M)	116.0 (3)		

(5) to 2.146 (5) Å (average 2.13 Å). These distances are in good agreement with the crystallographically characterized [*commo*-3,3′-Fe{3,1,2-$FeC_2B_9H_{11}$}$_2$][$N(CH_3)_4$]$_2$ and other ferracarboranes.[18] All interatomic distances of the icosahedral cage are within the normal range found in *closo*-MC_2B_9 complexes.[16]

As in the case of **15** the two icosahedra are bridged by a $-(CH_2)_4-$ chain which links C(01) and C(2)′.

Description of the Molecular Structure of 17b. The molecular structure of **17b** is presented in Figure 4, and Table IV lists selected interatomic distances and angles. The nickel atom is bound in an η^5 fashion to the five-membered face of each of two dicarbollide faces. The distance of the nickel atom to each mean plane of the dicarbollide cage faces is 1.48 Å, which is comparable to that observed in other nickelacarboranes.[19] Each of the bonding faces of the dicarbollide moieties is planar to within 0.023 (5) Å and staggered rather than eclipsed. Consequently, the bonding face of each icosahedral moiety nearly eclipses the lower belt of the other icosahedral fragment. Crystallographically characterized dicarbollide complexes which contain formal nickel(IV) have been observed to exist in a "cisoid" structure in which the polyhedral carbon atoms of the opposing ligand cages reside on the same side of the molecule in a staggered, nonslipped configuration. In the cisoid configuration the opposing ligands are tilted such that the carbon atoms are slightly more separated from one another than boron atoms on opposing ligand faces.[19] This tilt is reflected in the larger angle between normals to these two bonding planes, 13.6 (5)° for **17b** as compared to 9 (2)° for **15** and 8.7 (3)° for **16**, and may be due to the smaller ionic radius for nickel(IV) (0.62 Å) as compared to cobalt(III) and iron(III). The dicarbollide moieties are forced to bend inward toward the center of the molecule in order to bond with the smaller nickel atom. In addition, the bridging cages must twist with respect to the bridging group in order to provide an appropriate bonding distance to the metal. The result is that the carborane faces become staggered. Planes through lower belt [B(5)–B(6)–B(9)–B(11)–B(12)] atoms are nearly parallel to their respective bonding (or upper belt) faces, and atoms do not deviate by more than 0.006 (6) Å from their respective planes. Nickel–carbon distances range from 2.086 (5) to 2.158 (5) Å (average 2.12 Å), and nickel–boron distances range from 2.068 (6) to 2.112 (4) Å (average 2.09 Å). The numbers are in good agreement with previously characterized formal nickel(IV) carboranes.[19] All interatomic distances of the icosahedral cage are within the normal range found in *closo*-MC_2B_9 complexes.[16]

The two icosahedra are linked via a $-(CH_2)_4-$ chain which links C(02) and C(02). Complexes **15**, **16**, and **17b** have seven-membered rings. The torsion angles involving the four methylene carbon atoms are 77 (2), 75.7 (5), and 75.0 (5)°, respectively.

Conclusions

The complexes described in this paper comprise the first study of bridged and carbon-linked metallacarboranes. We are currently functionalizing these systems for later conjugation to monoclonal antibodies. The conjugates will then be evaluated as radiotransition-metal carriers for the antibody-mediated γ-imaging or β-therapy of tumors.

Experimental Section

General Considerations. Standard glovebox, Schlenk, and vacuum line techniques were employed for all manipulation of air- and moisture-sensitive compounds. Reaction solvents were reagent grade and distilled from appropriate drying agents under nitrogen before use. Tetrahydrofuran and diethyl ether were distilled from sodium benzophenone ketyl; benzene was distilled from potassium benzophenone ketyl. Deuteriated solvents were obtained from Cambridge Isotope Laboratories. Diethanolamine tritosylate was prepared by a literature method.[14] Triphenylmethylphosphonium bromide (Aldrich), *n*-butyllithium (2.5 M solution in hexanes) (Aldrich), and diethanolamine (Aldrich) were used as received. Cobalt(II) chloride (Cerac), nickel(II) bromide (Aldrich), chromium trichloride (Alfa), copper(II) chloride (Alfa), rhodium trichloride (Alfa), rhodium acetylacetonate (Alfa), and palladium(II) chloride (Alfa) were obtained in argon-filled vessels and were used without further purification. Ferrous chloride was prepared by the standard method described by Wilkinson.[20] Compound **1** was prepared as previously described.[6]

Physical Measurements. Proton (^{1}H NMR) and carbon (^{13}C NMR) spectra were obtained on a Bruker AF 200 instrument at 200.133 and 50.324 MHz, respectively. Boron (^{11}B NMR) spectra were obtained at 160.46 MHz on a Bruker AM 500 spectrometer. Chemical shifts for ^{1}H and ^{13}C NMR spectra were referenced to $SiMe_4$ (0.00 ppm) and measured with respect to residual protons in deuteriated solvents. Chemical shift values for ^{11}B spectra were referenced relative to external BF_3·OEt_2 (0.00 ppm). Resonances observed upfield of the reference compounds were assigned negative chemical shift values in all cases. Infrared spectra were obtained as Nujol mulls and were recorded on a Beckman FT-1100 instrument. Electron impact mass spectra were obtained on an AEI Ltd. Model MS-902 sector filled double-focusing spectrometer, and xenon FAB mass spectra were obtained on an AEI Ltd. Model MS-9 spectrometer.

1,1′-μ-1,3-C_3H_6-(2-$Si(CH_3)_2C(CH_3)_3$-1,2-$C_2B_{10}H_{10}$)$_2$ (2). To a solution of **1** (8.0 g, 30.9 mmol) in a benzene/diethyl ether (2:1) mixture (100 mL) at 0 °C was added a 2.5 M solution of *n*-BuLi in hexane (13.6 mL, 34.0 mmol) dropwise with stirring. The mixture was allowed to stir for 30 min at ambient temperature. The solution was then cooled to 0 °C, and 1,3-dibromopropane (1.7 mL, 17.0 mmol) was added dropwise with stirring. After being refluxed for 5 h the solution was quenched with 30 mL of water, transferred to a separatory funnel, and diluted with 100 mL of diethyl ether. The layers were separated, and the aqueous layer was extracted with additional Et_2O (2 × 200 mL). The combined filtrates were then dried over anhydrous Mg_2SO_4 and concentrated in vacuo. The white solids were washed with petroleum ether and the insoluble solids **2** collected in 61% yield (5.2 g, 9.4 mmol), mp 195–196 °C. IR (Nujol, cm^{-1}): 2928 (s), 2583 (s), 1259 (s), 1087 (m), 840 (s), 820 (s). ^{1}H NMR ($CDCl_3$): 2.13 (m, 4 H, α-CH_2), 1.78 (m, 2 H,

(19) St. Clair, D.; Zalkin, A.; Templeton, D. H. *J. Am. Chem. Soc.* **1970**, *92*, 1173.

(20) Wilkinson, G. *Org. Synth.* **1961**, *36*, 31.

β-CH_2), 1.05 (s, 18 H, $C(CH_3)_3$), 0.31 (s, 12 H, CH_3). ^{13}C NMR ($CDCl_3$): 80.2, 76.1, 36.8, 30.5, 27.5, 20.4, –2.4. ^{11}B NMR (chloroform): –0.09 (d, 2 B), –4.21 (d, 2 B), –7.83 (d, 4 B), –10.77 (d, 12 B). MS: Theoretical ion distribution for $C_{19}H_{56}{}^{11}B_{20}Si_2$ centered around m/e 557.05; observed ion distribution centered around m/e 557. Anal. Calcd for $C_{19}H_{56}B_{20}Si_2$: C, 40.97; H, 10.13; B, 38.82; Si, 10.08. Found: C, 40.78; H, 9.86; B, 39.00; Si, 9.89.

1,1′-μ-1,3-C_3H_6-(1,2-$C_2B_{10}H_{11}$)$_2$ (3). A solution of **2** (2.5 g, 4.5 mmol) in dry THF (100 mL) was cooled to –76 °C, and a 1.0 M solution of tetrabutylammonium fluoride in THF (9.2 mL, 9.2 mmol) was added dropwise with stirring. The mixture was allowed to stir for 30 min. After the solution was warmed to room temperature, 20 mL of water was added. The solution was diluted with 100 mL of diethyl ether and transferred to a separatory funnel. The layers were separated and the aqueous layer was extracted with additional Et_2O (2 × 100 mL). The combined extracts were dried over anhydrous Mg_2SO_4 and concentrated in vacuo. The white solids were washed with petroleum ether, and the insoluble solid **3** was collected in 88% yield (1.3 g, 4.0 mmol), mp >285 °C. IR (Nujol, cm^{-1}): 2916 (s), 2579 (s), 1126 (w), 1016 (w), 1000 (w), 723 (s). ^1H NMR ($(CD_3)_2CO$): 4.62 (s, 2 H, Cb C–H), 2.37 (m, 4 H, J_{HH} = 8.4, α-CH_2), 1.75 (m, 2 H, β-CH_2). ^{13}C NMR ($(CD_3)_2CO$): 76.0, 62.9, 36.8, 29.5. ^{11}B NMR (acetone): –2.42 (d, 2 B), –5.56 (d, 2 B), –9.21 (d, 4 B), –11.05 (d, 4 B), –11.44 (d, 4 B), –12.59 (d, 4 B). MS: Theoretical ion distribution for $C_7H_{28}B_{20}$ centered around m/e 328.52; observed ion distribution centered around m/e 329. Anal. Calcd for $C_7H_{28}B_{20}$: C, 25.59; H, 8.59; B, 65.82. Found: C, 25.81; H, 8.39; B, 65.51.

[7,7′-μ-1,3-C_3H_6-(7,8-$C_2B_9H_{11}$)$_2$]$^{2-}$,2Cs^+ (4). To a solution of **3** (1.2 g, 3.7 mmol) in 95% ethanol (40 mL) was added potassium hydroxide (pellets, 1.4 g, 24.4 mmol). The solution was heated at reflux overnight and cooled, and CO_2 (1.6 g, 37.0 mmol) was added. The potassium carbonate was separated by filtration and washed with ethanol (3 × 50 mL), and the filtrates were concentrated in vacuo. The crude solids were dissolved in water (20 mL), and the mixture was added to an aqueous solution of cesium chloride (1.6 g, 9.3) mmol). The solids were filtered out, dried, and recrystallized from hot water to give **4** in 61% yield (1.3 g, 2.2 mmol), mp >285 °C. IR (Nujol, cm^{-1}): 2908 (s), 2528 (s), 1036 (s), 1000 (w), 733 (s). ^1H NMR ($(CD_3)_2CO$): 1.62 (s, 2 H, Cb C–H), 1.45 (m, 6 H, CH_2). ^{13}C NMR ($(CD_3)_2CO$): 60.3, 47.9, 40.6, 40.5, 33.8, 33.6. ^{11}B NMR (acetone): –10.72 (d, 4 B), –13.72 (d, 2 B), –17.66 (d, 6 B), –22.25 (d, 2 B), –33.20 (d, 2 B), –37.08 (d, 2 B). MS (negative ion FAB): Theoretical ion distribution for $C_7H_{28}B_{18}$ centered around m/e 306.90; observed ion distribution centered around m/e 306.42. Anal. Calcd for $C_7H_{28}B_{18}Cs_2$: C, 14.68; H, 4.93; B, 33.98. Found: C, 14.41; H, 4.84; B, 33.75.

1,1′-μ-1,4-C_4H_8-(2-$Si(CH_3)_2C(CH_3)_3$-1,2-$C_2B_{10}H_{10}$)$_2$ (5). To a solution of **1** (10.0 g, 38.7 mmol) in benzene/diethyl ether (2:1) mixture (100 mL) at 0 °C was added a 2.5 M solution of *n*-BuLi in hexane (17.0 mL, 42.6 mmol) dropwise with stirring. The mixture was allowed to stir for 30 min at ambient temperature. The solution was cooled to 0 °C, and a solution of 1,4-dibromobutane (3.5 mL, 29.0 mmol) in a benzene/diethyl ether (2:1) mixture (5 mL) was added dropwise with stirring. After being refluxed overnight, the solution was quenched with 75 mL of water, transferred to a separatory funnel, and diluted with 200 mL of diethyl ether. The layers were separated, and the aqueous layer was extracted with additional Et_2O (2 × 200 mL). The combined filtrates were then dried over anhydrous $MgSO_4$ and concentrated in vacuo. The crude white solids were washed with petroleum ether, and the residual solids **5** were collected in 70% yield (7.7 g, 13.5 mmol), mp 194–196 °C. IR (Nujol, cm^{-1}): 2914 (s), 2598 (s), 1262 (s), 1077 (s), 838 (s), 820 (s), 730 (s). ^1H NMR ($CDCl_3$): 2.17 (t, 4 H, α-CH_2), 1.42 (m, 4 H, β-CH_2), 1.06 (s, 18 H), $C(CH_3)_3$), 0.32 (s, 12 H, CH_3). ^{13}C NMR ($CDCl_3$): 80.7, 76.3, 37.5, 29.7, 27.6, 20.4, –2.4. ^{11}B NMR (acetone): –0.14 (d, 2 B), –4.17 (d, 2 B), –7.71 (d, 4 B), –10.65 (d, 12 B). MS: Theoretical ion distribution for ($C_{20}H_{58}B_{20}Si_2 - C_4H_9$) centered around m/e 513.96; observed ion distribution centered around m/e 515. Anal. Calcd for $C_{20}H_{58}B_{20}Si_2$: C, 42.06; H, 10.24; B, 37.86. Found: C, 41.80; H, 10.09; B, 37.64.

1,1-μ-1,4-C_4H_8-(1,2-$C_2B_{10}H_{11}$)$_2$ (6). A solution of **5** (7.7 g, 13.5 mmol) in dry THF (75 mL) was cooled to –76 °C, and a 1.0 M solution of tetrabutylammonium fluoride in THF (27.8 mL, 27.8 mmol) was added dropwise with stirring. The mixture was allowed to stir for 30 min while being warmed to room temperature, and then 40 mL of water was added. The solution was diluted with 200 mL of diethyl ether and transferred to a separatory funnel. The layers were separated, and the aqueous layer was extracted with additional Et_2O (2 × 100 mL). The combined extracts were dried over anhydrous $MgSO_4$ and concentrated in vacuo. The white solids were washed with petroleum ether, and the nonsoluble solids **6** were collected in 92% yield (4.3 g, 12.5 mmol), mp >285 °C. IR (Nujol, cm^{-1}): 2916 (s), 2556 (s), 1121 (w), 1069 (m), 1018 (m), 1002 (w), 723 (s). ^1H NMR ($(CD_3)_2CO$): 4.55 (s, 2 H, Cb C–H), 2.35 (m, 4 H, α-CH_2), 1.51 (m, 4 H, β-CH_2). ^{13}C NMR ($(CD_3)_2CO$): 76.5, 63.1, 37.5, 29.1. ^{11}B NMR (acetone): –2.52 (d, 2 B), –5.70 (d, 2 B), –9.26 (d, 4 B), –11.17 (d, 8 B), –12.67 (d, 4 B). MS (high resolution): Theoretical ion distribution for $C_8H_{30}B_{20}$ centered around m/e 342.54; observed ion distribution centered around m/e 342.54. Anal. Calcd for $C_8H_{30}B_{20}$: C, 28.05; H, 8.83; B, 63.12. Found: C, 28.30; H, 8.59; B, 62.92.

[7,7′-μ-1,4-C_4H_8-(7,8-$C_2B_9H_{11}$)$_2$]$^{2-}$,2Cs^+ (7). To a solution of **6** (4.3 g, 12.5 mmol) in 95% ethanol (75 mL) was added potassium hydroxide (pellets, 3.5 g, 62.5 mmol). The solution was allowed to reflux overnight and cooled, and CO_2 (5.5 g, 125 mmol) was added. The resulting potassium carbonate was filtered out and washed with ethanol (3 × 50 mL) and concentrated in vacuo. The crude solids were dissolved in water (50 mL), and the mixture was added to an aqueous solution of cesium chloride (5.3 g, 31.3 mmol). The solids were filtered out, dried, and recrystallized from hot water to give **7** in 80% yield (5.8 g, 9.0 mmol), mp >285 °C. IR (Nujol, cm^{-1}): 2949 (s), 2528 (s), 1034 (m), 998 (m), 735 (w). ^1H NMR ($(CD_3)_2CO$): 1.62 (s, 2 H, Cb C–H), 1.47 (m, 8 H), CH_2). ^{13}C NMR ($(CD_3)_2CO$): 59.8, 47.5, 40.3, 32.2. ^{11}B NMR (acetone): –10.81 (d, 4 B), –13.77 (d, 2 B), –17.87 (d, 6 B), –22.22 (d, 2 B), –33.22 (d, 2 B), –37.09 (d, 2 B). MS (negative ion FAB): Theoretical ion distribution for $C_8H_{30}B_{18}$ centered around m/e 320.92; observed ion distribution centered around m/e 320.42. Anal. Calcd for $C_8H_{30}B_{18}Cs_2$: C, 16.38; H, 5.15; B, 33.17. Found: C, 16.13; H, 5.01; B, 33.10.

1,1′-μ-1,5-C_5H_{10}-(2-$Si(CH_3)_2C(CH_3)_3$-1,2-$C_2B_{10}H_{10}$)$_2$ (8). To a solution of **1** (5.0 g, 19.3 mmol) in a benzene/diethyl ether (2:1) mixture (100 mL) at 0 °C was added a 2.5 M solution of *n*-BuLi in hexane (8.5 mL, 21.3 mmol) dropwise with stirring. The mixture was allowed to stir for 30 min at ambient temperature. The solution was cooled to 0 °C, and 1,5-dibromopentane (1.5 mL, 10.6 mmol) was added dropwise with stirring. After being heated at reflux overnight, the solution was quenched with 20 mL of water, transferred to a separatory funnel, and diluted with 100 mL of diethyl ether. The layers were separated, and the aqueous layer was extracted with additional Et_2O (2 × 200 mL). The combined extracts were then dried over anhydrous $MgSO_4$ and concentrated in vacuo. The light orange solids were washed with petroleum ether, and the insoluble solids **8** were collected in 53% yield (3.0 g, 5.1 mmol), mp 171–173 °C. IR (Nujol, cm^{-1}): 2908 (s), 2572 (s), 1256 (m), 1065 (s), 838 (m), 818 (m), 795 (w). ^1H NMR ($CDCl_3$): 2.16 (t, 4 H, α-CH_2), 1.51 (m, 4 H, β-CH_2), 1.18 (m, 2 H, γ-CH_2), 1.06 (s, 18 **H**, $C(CH_3)_3$), 0.32 (s, 12 H, CH_3). ^{13}C NMR ($CDCl_3$): 81.1, 76.3, 37.6, 29.8, 28.7, 27.6, 20.4, –2.4. ^{11}B NMR (chloroform): –0.23 (d, 2 B), –4.35 (d, 2 B), –7.84 (d, 4 B), –10.77 (d, 12 B). MS (FAB): Theoretical ion distribution centered around m/e 585.10; observed ion distribution centered around m/e 585. Anal. Calcd for $C_{21}H_{60}B_{20}Si_2$: C, 43.11; H, 10.34; B, 36.95. Found: C, 43.18; H, 10.11; B, 36.78.

1,1-μ-1,5-C_5H_{10}-(1,2-$C_2B_{10}H_{11}$)$_2$ (9). A solution of **8** (2.7 g, 4.5 mmol) in dry THF (100 mL) was cooled to –76 °C, and a 1.0 M solution of tetrabutylammonium fluoride in THF (9.3 mL, 9.3 mmol) was added dropwise with stirring. The mixture was allowed to stir 30 min at room temperature, and 20 mL of water was added. The solution was diluted with 100 mL of diethyl ether and transferred to a separatory funnel. The layers were separated, and the aqueous layer was extracted with additional Et_2O (2 × 100 mL). The combined extracts were dried over anhydrous $MgSO_4$ and concentrated in vacuo. The white solids were washed with petroleum ether, and the insoluble solids **9** were collected in 88% yield (1.4 g, 4.0 mmol), mp 177–179 °C. IR (Nujol, cm^{-1}): 2911 (s), 2582 (s), 1209 (w), 1126 (w), 1066 (m), 1018 (m), 1003 (w), 938 (w), 724 (s). ^1H NMR ($(CD_3)_2CO$): 4.51 (s, 2 H, Cb C–H), 2.31 (t, 4 H, J_{HH} = 8.5, α-CH_2), 1.52 (m, 4 H, β-CH_2), 1.28 (m, 2 H, γ-CH_2). ^{13}C NMR ($(CD_3)_2CO$): 76.8, 63.0, 37.9, 29.4, 28.7. ^{11}B NMR (acetone): –2.57 (d, 2 B), –5.78 (d, 2 B), –9.30 (d, 4 B), –11.12 (d, 4 B), –11.49 (d, 4 B), –12.72 (d, 4 B). MS: Theoretical ion distribution for $C_9H_{32}B_{20}$ centered around m/e 356.57; observed ion distribution centered around m/e 357. Anal. Calcd for $C_9H_{32}B_{20}$: C, 30.32; H, 9.04; B, 60.64. Found: C, 30.29; H, 8.83; B, 60.41.

[7,7′-μ-1,5-C_5H_{10}-(7,8-$C_2B_9H_{11}$)$_2$]$^{2-}$,2Cs^+ (10). To a solution of **9** (1.3 g, 3.7 mmol) in 95% ethanol (40 mL) was added potassium hydroxide (pellets, 1.4 g, 24.4 mmol). The solution was heated to reflux overnight and cooled, and CO_2 (1.6 g, 37.0 mmol) was added. The resulting potassium carbonate was filtered out and washed with ethanol (3 × 50 mL) and concentrated in vacuo. The crude solids were dissolved in water (20 mL) and added to an aqueous solution of cesium chloride (1.6 g, 9.2

mmol). The solids were filtered out, dried, and recrystallized from hot water to give **10** in 54% yield (1.2 g, 2.0 mmol), mp >270 °C. IR (Nujol, cm^{-1}): 2918 (s), 2512 (s), 1031 (m), 1003 (w), 728 (w). ^1H NMR (CD_3OD): 0.82 (s, 2 H, Cb C–H), 0.33–0.22 (m, 10 H, CH_2). ^{13}C NMR (CD_3OD): 60.6, 47.7, 39.2, 30.8, 29.7, 29.6. ^{11}B NMR (acetone): −11.33 (d, 4 B), −13.86 (d, 2 B), −17.85 (d, 6 B), −22.15 (d, 2 B), −33.53 (d, 2 B), −37.44 (d, 2 B). MS (negative ion FAB): Theoretical ion distribution for $C_9H_{32}B_{18}$ centered around *m/e* 334.95; observed ion distribution centered around *m/e* 334.49. Anal. Calcd for $C_9H_{32}B_{18}Cs_2$: 17.99; H, 5.37; B, 32.39. Found: C, 17.68; H, 5.19; B, 31.94.

1,1′-μ-TosN(CH$_2$CH$_2$–)$_2$-(2-Si(CH$_3$)$_2$C(CH$_3$)$_3$-1,2-C$_2$B$_{10}$H$_{10}$)$_2$ (11). To a solution of **1** (15.0 g, 58.2 mmol) in a benzene/diethyl ether (2:1) mixture (150 mL) at 0 °C was added a 2.5 M solution of *n*-BuLi in hexane (25.6 mL, 64.0 mmol) dropwise with stirring. The mixture was allowed to stir for 30 min to ambient temperature. The solution was cooled to 0 °C, and a solution of diethanolamine tritosylate[14] (13.2 mL, 32.0 mmol) in a benzene/diethyl ether (2:1) mixture (100 mL) was added dropwise with stirring. After being heated to reflux overnight the solution was quenched with 50 mL of water, transferred to a separatory funnel, and diluted with diethyl ether (100 mL). The layers were separated, and the aqueous layer was extracted with additional Et_2O (3 × 50 mL). The combined filtrates were then dried over anhydrous Mg_2SO_4 and concentrated in vacuo. To the resulting oil was added pentane (100 mL) and the nonsoluble white solids **11** were collected in 17% yield (3.7 g, 5.0 mmol), mp 152–154 °C. IR (Nujol, cm^{-1}): 3042 (w), 2908 (s), 2576 (s), 1625 (w), 1599 (w), 1451 (s), 1375 (m), 1344 (s), 1264 (s), 1044 (m), 987 (s), 930 (w), 839 (m), 815 (s), 797 (m), 777 (m), 739 (s), 651 (m). ^1H NMR ($(CD_3)_2CO$): 7.76 (d, 2 H, J_{HH} = 8.2, phenyl C–H), 7.49 (d, 2 H, J_{HH} = 8.2, phenyl C–H), 3.34 (m, 4 H, CH_2), 2.60 (m, 4 H, CH_2), 2.45 (s, 3 H, tolyl CH_3), 1.09 (s, 18 H, $C(CH_3)_3$), 0.39 (s, 12 H, CH_3). ^{13}C NMR ($CDCl_3$): 145.0, 136.7, 130.9, 127.8, 79.2, 77.2, 49.6, 37.4, 27.8, 21.3, 20.8, −2.5. ^{11}B NMR (chloroform): 0.72 (d, 2 B), −3.18 (d, 2 B), −7.13 (d, 4 B), −9.72 (d, 12 B). MS: Theoretical ion distribution for $C_{27}H_{65}B_{20}Si_2N_1S_1O_2 - C_4H_9$ centered around *m/e* 683; observed ion distribution centered around *m/e* 686.

1,1′-μ-TosN(CH$_2$CH$_2$–)$_2$-(1,2-C$_2$B$_{10}$H$_{11}$)$_2$ (12). A solution of **11** (3.4 g, 4.6 mmol) in dry THF (100 mL) was cooled to −76 °C, and a 1.0 M solution of tetrabutylammonium fluoride in THF (13.3 mL, 13.3 mmol) was added dropwise with stirring. The mixture was allowed to stir for 30 min at room temperature whereupon 20 mL of water was added. The solution was diluted with 100 mL of diethyl ether and transferred to a separatory funnel. The layers were separated, and the aqueous layer was extracted with additional Et_2O (2 × 100 mL). The combined extracts were dried over anhydrous Mg_2SO_4 and concentrated in vacuo, and the resulting white solids **12** were collected in 99% yield (2.3 g, 4.6 mmol), mp >204 °C. IR (Nujol, cm^{-1}): 3040 (w), 2950 (s), 2584 (s), 1340 (s), 1160 (s), 965 (m), 725 (s), 650 (m). ^1H NMR ($(CD_3)_2CO$): 7.74 (d, 2 H, J_{HH} = 8.2, phenyl C–H), 7.45 (d, 2 H, J = 8.1, phenyl C–H), 4.69 (s, 2 H, Cb C–H), 3.32 (m, 4 H, CH_2), 2.63 (m, 4 H, CH_2), 2.14 (s, 3 H, CH_3). ^{13}C NMR ($(CD_3)_2CO$): 144.8, 136.6, 130.8, 127.8, 73.5, 63.4, 48.4, 36.8, 21.3. ^{11}B NMR (acetone): −2.38 (d, 2 B), −5.17 (d, 2 B), −9.08 (d, 4 B), −11.35 (d, 8 B), −12.51 (d, 4 B). MS: Theoretical ion distribution for $C_{15}H_{37}B_{20}N_1S_1O_2$ centered around *m/e* 511.75; observed ion distribution centered around *m/e* 511.52.

1,1′-μ-TosN(CH$_2$CH$_2$–)$_2$-(7,8-C$_2$B$_9$H$_{11}$)$_2$]$^{2-}$,2Cs$^+$ (13). To a solution of **12** (2.0 g, 3.9 mmol) in 95% ethanol (75 mL) was added potassium hydroxide (pellets, 1.1 g, 19.5 mmol). The solution was allowed to reflux overnight and cooled, and CO_2 (1.7 g, 39 mmol) was added. The resulting potassium carbonate was filtered out, washed with ethanol (3 × 50 mL), and concentrated in vacuo. The crude solids were dissolved in water (10 mL) and added to an aqueous solution of cesium chloride (1.5 g, 8.6 mmol). The solids were filtered out, dried, and recrystallized from hot water to give a yellow solid **13** in 47% yield (1.4 g, 1.9 mmol), decomposn pt >170 °C. IR (Nujol, cm^{-1}): 3029 (w), 2905 (s), 2512 (s), 1597 (s), 1319 (s), 1155 (s), 1085 (m), 1031 (m), 813 (m), 723 (m), 653 (m). ^1H NMR ($(CD_3)_2CO$): 7.66 (d, 2 H, J_{HH} = 8.0, phenyl C–H), 7.38 (d, 2 H, J_{HH} = 7.9, phenyl C–H), 3.19 (m, CH_2, Cb C–H), 2.39 (s, 3 H, CH_3), 1.67 (m, 2 H, CH_2). ^{13}C NMR ($(CD_3)_2CO$): 143.6, 137.8, 130.1, 127.3, 57.2, 49.5, 49.4, 46.0, 38.6, 21.1. ^{11}B NMR (acetone): −10.59 (d, 4 B), −13.67 (d, 2 B), −15.98 (d, 2 B), −18.58 (d, 4 B), −21.55 (d, 2B), −32.90 (d, 2 B), −36.96 (d, 2 B). MS (negative ion FAB): Theoretical ion distribution for $C_{15}H_{37}B_{18}SO_2N$ centered around *m/e* 490.13. Observed ion distribution centered around *m/e* 489. Anal. Calcd for $C_{15}H_{37}B_{18}SO_2NCs_2$: C, 23.83; H, 4.93; B, 25.74. Found: C, 24.71; H, 5.13; B, 26.60.

[7,7′-μ-1,3-C$_3$H$_6$-(7,8-C$_2$B$_9$H$_{10}$)$_2$Co]$^-$(C$_6$H$_5$)$_3$PCH$_3^+$ (14). A solution of **4** (1.0 g, 1.8 mmol) in tetrahydrofuran (80 mL) at 25 °C was slowly added to a suspension of NaH (0.17 g, 7.2 mmol) in THF (30 mL) dropwise with stirring. The reaction mixture was stirred at reflux temperature for 4 h. When the excess sodium hydride had settled, the clear solution was decanted and then added to a suspension of anhydrous cobalt chloride (0.6 g, 4.2 mmol) in dry tetrahydrofuran (50 mL) to produce a black solution. This solution was refluxed overnight, cooled, and filtered to remove cobalt metal, LiCl, and CsCl. After removal of the solvent in vacuo, the residue was extracted with hot water, the resulting aqueous solution was filtered, and the orange filtrate was treated with triphenylmethylphosphonium bromide (0.9 g, 2.4 mmol). The triphenylmethylphosphonium salt formed was extracted with methylene chloride and chromatographed (SiO_2) with 80:20 ethyl acetate/hexane without separation of isomers. The product was recrystallized from a methylene chloride/hexane solution to give orange platelets of **14** (531 mg, 46% yield), mp 216–218 °C. IR (Nujol, cm^{-1}): 3029 (s), 2911 (s), 2546 (m), 1165 (w), 1113 (w), 1031 (w), 998 (w), 895 (w), 741 (w), 720 (w), 687 (w). ^1H NMR ($(CD_3)_2CO$): 7.87 (m, 15 H, phenyl C–H), 3.90 (sb, 1 H, Cb C–H), 3.79 (sb, 1 H, Cb C–H), 3.24 (s, 3 H, CH_3), 3.17 (s, 3 H, CH_3), 2.46 (m, 4 H, α-CH_2), 1.81 (m, 2 H, β-CH_2). ^{13}C NMR ($(CD_3)_2CO$): 135.7, 134.1, 133.9, 131.1, 130.8, 38.8, 34.7, 14.0. ^{11}B NMR (acetone): 7.15 (d), 5.59 (d), 1.46 (d), −2.73 (d), −3.83 (d), −6.57 (d), −12.30 (d), −16.51 (d), −17.43 (d). MS (negative ion FAB): Theoretical ion distribution for $C_7H_{26}B_{18}Co$ centered around *m/e* 363.82; observed ion distribution centered around *m/e* 362. Anal. Calcd for $C_{26}H_{44}B_{18}CoP$: C, 48.70; H, 6.92; Co, 9.19. Found: C, 48.45; H, 6.73; Co, 9.06.

[7,7′-μ-1,4-C$_4$H$_8$-(7,8-C$_2$B$_9$H$_{10}$)$_2$Co]$^-$(C$_6$H$_5$)$_3$PCH$_3^+$ (15). A solution of **7** (1.1 g, 2.0 mmol) in dry tetrahydrofuran (80 mL) at 25 °C was slowly added to a suspension of NaH (0.19 g, 8.0 mmol) in THF (30 mL) with stirring. The reaction mixture was stirred at the reflux temperature for 4 h. When the excess sodium hydride had settled, the clear solution was decanted and then added to a suspension of anhydrous cobalt chloride (0.47 g, 4.0 mmol) in dry tetrahydrofuran (50 mL). The black solution was refluxed overnight, cooled, and filtered to remove cobalt metal, LiCl, and CsCl. After removal of the solvent in vacuo, the residue was extracted with hot water, the resulting aqueous solution was filtered, and the orange filtrate was treated with triphenylmethylphosphonium bromide (1.0 g, 3.0 mmol). The crude solid formed was extracted with methylene chloride and chromatographed (SiO_2) with 80:20 ethyl acetate/hexane without separation of isomers. The product was recrystallized from a methylene chloride/hexane solution to afford orange platelets of **15** (800 mg, 61% yield), mp 176–179 °C. IR (Nujol, cm^{-1}): 3029 (s), 2911 (s), 2546 (m), 1165 (w), 1113 (w), 1031 (w), 998 (w), 895 (w), 741 (w), 720 (w), 687 (w). ^1H NMR ($(CD_3)_2CO$): 7.82 (m, 15 H, phenyl C–H), 3.68 (s, 2 H, Cb C–H), 3.17 (dd, 6 H, J_{PH} = 14.1, CH_3), 2.68 (m, 4 H, α-CH_2), 1.73 (m, 4 H, β-CH_2). ^{13}C NMR ($(CD_3)_2CO$): 135.6, 134.1, 131.1, 130.9, 58.5, 55.3, 45.5, 27.8, 9.2. ^{11}B NMR (acetone): 7.20 (d), 6.46 (d), 5.57 (d), 1.81 (d), −1.79 (d), −3.20 (d), −4.03 (d), −5.69 (d), −6.90 (d), −7.52 (d), −7.96 (d), −9.85 (d), −14.54 (d), −16.06 (d), −17.35 (d), −18.00 (d), −19.66 (d). MS (negative ion FAB): Theoretical ion distribution for $C_8H_{28}B_{18}CoP$ centered around *m/e* 377.84; observed ion distribution centered around *m/e* 378. Anal. Calcd for $C_{27}H_{46}B_{18}CoP$: C, 49.50; H, 7.08; B, 29.7; Co, 9.00. Found: C, 49.25; H, 6.94; B, 29.59; Co, 8.78.

[7,7′-μ-1,4-C$_4$H$_8$-(7,8-C$_2$B$_9$H$_{10}$)$_2$Fe]$^-$(C$_6$H$_5$)$_3$PCH$_3^+$ (16). A solution of **7** (0.9 g, 1.5 mmol) in dry tetrahydrofuran (70 mL) at 25 °C was slowly added to a suspension of NaH (0.14 g, 6.0 mmol) in THF (25 mL) dropwise with stirring. The reaction mixture was stirred at reflux temperature for 4 h. When the excess sodium hydride had settled, the clear solution was decanted and then added to a suspension of ferrous chloride (0.4 g, 3.0 mmol) in dry tetrahydrofuran (50 mL). The red solution was refluxed overnight, cooled, and filtered to remove iron metal, LiCl, and CsCl. After removal of the solvent in vacuo, the residue was extracted with hot water, the resulting aqueous solution was filtered, and the red filtrate was treated with triphenylmethylphosphonium bromide (0.9 g, 2.5 mmol). The crude solid formed was extracted with methylene chloride and chromatographed (SiO_2) with 80:20 ethyl acetate/hexane without separation of isomers. The product was recrystallized from a methylene chloride/hexane solution to afford red parallelepipeds of **16** (401 mg, 41% yield), mp 158–160 °C. IR (Nujol, cm^{-1}): 3041 (w), 2920 (s), 2551 (s), 1160 (w), 1114 (m), 1072 (w), 991 (m), 967 (w), 875 (m), 722 (m). ^{11}B NMR (acetone): 104.30, 96.94, 33.64, 29.97, 22.10, 20.34, 18.09, 10.10, 4.80, 2.40, −2.22, −8.85, −15.62, −23.13, −25.06, −28.87, −35.12, −247.49, −328.89, −422.78, −464.63, −498.68, −512.83. MS (negative ion FAB): Theoretical ion distribution for $C_8H_{28}B_{18}Fe$ centered around

m/e 374.76; observed ion distribution centered around m/e 375. Anal. Calcd for $C_{27}H_{46}B_{18}FeP$: C, 49.73; H, 7.11; Fe, 8.56. Found: C, 49.64; H, 7.21; Fe, 8.30.

[7,7′-μ-1,4-C_4H_8-(7,8-$C_2B_9H_{10}$)$_2$]Ni (17b). A solution of **7** (1.0 g, 1.8 mmol) in dry tetrahydrofuran (75 mL) at 25 °C was slowly added to a suspension of NaH (0.17 g, 7.2 mmol) in THF (30 mL) dropwise with stirring. The reaction mixture was stirred at reflux temperature for 4 h. When the excess sodium hydride had settled, the clear solution was decanted and then added to a suspension of anhydrous nickel dibromide (0.8 g, 3.6 mmol) in dry tetrahydrofuran (50 mL). The resulting green solution was refluxed overnight, cooled, and filtered to remove nickel metal, CsCl, and LiCl. After removal of the solvent in vacuo, the residue was extracted with hot water, the resulting aqueous solution filtered, and the green filtrate treated with triphenylmethylphosphonium bromide (0.9 g, 2.4 mmol). The crude solid formed was extracted with methylene chloride and chromatographed (SiO_2) with 80:20 ethyl acetate/hexane without separation of isomers. The green residue (**17a**) was dissolved in a 1:1 water/acetonitrile (60 mL) solution, the mixture was warmed to 50 °C, and a solution (10 mL) of $FeCl_3$ (0.3 g, 1.8 mmol) was added slowly. After 30 min the orange solution was cooled, acetonitrile was removed in vacuo, and the suspended orange solid was extracted with diethyl ether (3 × 100 mL). The solvent was removed in vacuo, and the residue was chromatographed (SiO_2) with 50:50 benzene/hexane without separation of isomers. The product was recrystallized from a methylene chloride/hexane solution to afford orange crystals of **17b** (394 mg, 58% yield), dec >200 °C. IR (Nujol, cm^{-1}): 2905 (s), 2523 (s). ^1H NMR ($(CD_3)_2CO$): 5.18 (s, 1 H), 5.02 (s, 1 H), 2.86 (s, 4 H), 1.70 (m, 4 H). ^{13}C NMR ($(CD_3)_2CO$): 55.21, 45.2, 34.6, 27.2. ^{11}B NMR (acetone): 20.92, (d, 2 B), 16.93 (d, 2 or 4 B), 3.30 (d, 4 or 6 B), –0.31 (d, 4 or 6 B), –7.74 (d, 2 B), –13.88 (d, 2 B). MS (negative ion FAB): Theoretical ion distribution for $C_8H_{28}B_{18}Ni$ centered around m/e 377.62; observed ion distribution centered around m/e 377. Anal. Calcd for $C_8H_{28}B_{18}Ni$: C, 25.45; H, 7.47. Found: C, 25.24; H, 7.29.

[7,7′-μ-1,4-C_4H_8-(7,8-$C_2B_9H_{10}$)$_2$Cr]$^-$(C_6H_5)$_3$$PCH_3^+$ (18). A solution of **7** (0.9 g, 1.5 mmol) in dry tetrahydrofuran (75 mL) at 0 °C was slowly added to a solution of NaH (0.14, 6.0 mmol) in THF (30 mL) dropwise with stirring. The reaction mixture was stirred at reflux temperature for 4 h. When the excess sodium hydride had settled, the clear solution was decanted and then added to a suspension of anhydrous chromium trichloride (0.47 g, 3.0 mmol) in dry tetrahydrofuran (80 mL). The red solution was refluxed overnight, cooled, and filtered to remove the chromium metal and lithium chloride. After removal of the solvent in vacuo, the residue was extracted with hot water, the resulting aqueous solution was filtered, and the red filtrate was treated with triphenylmethylphosphonium bromide (0.9 g, 2.5 mmol). The crude solid formed was extracted with methylene chloride and chromatographed (SiO_2) with 80:20 ethyl acetate/hexane without separation of isomers to afford **18** (380 mg, 39% yield), mp 52–56 °C. IR (Nujol, cm^{-1}): 3042 (w), 2920 (s), 2533 (s), 1114 (m), 1069 (w), 990 (m), 894 (m), 737 (m), 722 (m), 686 (m). ^{11}B NMR (acetone): 141.98, 11.02, –45.65, –64.77, –93.39, –113.60, –164.38. MS (negative ion FAB): Theoretical ion distribution for $C_8H_{28}B_{18}Cr$ centered around m/e 370.91; observed ion distribution centered around m/e 371.

[7,7′-μ-1,5-C_5H_{10}-(7,8-$C_2B_9H_{10}$)$_2$Co]$^-$(C_6H_5)$_3$$PCH_3^+$ (19). A solution of **10** (0.5 g, 0.9 mmol) in dry tetrahydrofuran (75 mL) at 0 °C was slowly added to a solution of NaH (0.09 g, 3.6 mmol) in THF (10 mL) dropwise with stirring. The reaction mixture was stirred at reflux temperature for 4 h. When the excess sodium hydride had settled, the clear solution was decanted and then added to a suspension of anhydrous cobalt chloride (0.3 g, 2.1 mmol) in dry tetrahydrofuran (75 mL). The black solution was refluxed overnight, cooled, and filtered to remove the cobalt metal and lithium chloride. After removal of the solvent in vacuo, the residue was extracted with hot water, the resulting aqueous solution was filtered, and the orange filtrate was treated with triphenylmethylphosphonium bromide (0.6 g, 1.8 mmol). The crude solid formed was extracted with methylene chloride and chromatographed (SiO_2) with 80:20 ethyl acetate/hexane without separation of isomers to afford an orange solid **19** (120 mg, 21% yield), mp 50–52 °C. IR (Nujol, cm^{-1}): 2920 (s), 2558 (s), 1116 (w), 1067 (w), 995 (w), 895 (w), 720 (w), 681 (w). ^1H NMR ($(CD_3)_2CO$): 7.87 (m, 15 H, phenyl C–H), 3.85 (sb, 2 H, Cb C–H), 3.25 (s, 3 H, CH_3), 3.18 (s, 3 H, CH_3), 1.76 (m, 4 H, α-CH_2), 1.47 (m, 4 H, β-CH_2). ^{11}B NMR (acetone): 6.41 (d), 0.19 (d), –5.57 (d), –6.99 (d), –9.04 (d), –15.73 (d), –20.03 (d). MS (negative ion FAB): Theoretical ion distribution for $C_9H_{30}B_{18}Co$ centered around m/e 391.87; observed ion distribution centered around m/e 391.

[7,7′-μ-TosN(CH_2CH_2–)$_2$-(7,8-$C_2B_9H_{10}$)$_2$Co]$^-$(C_6H_5)$_3$$PCH_3^+$ (20). A solution of **13** (0.6 g, 0.8 mmol) in dry tetrahydrofuran (75 mL) at 25 °C was slowly added a solution of NaH (0.08 g, 3.2 mmol) dropwise with stirring. The reaction mixture was stirred at reflux temperature for 4 h. When the excess sodium hydride had settled, the clear solution was decanted and then added to a suspension of anhydrous cobalt chloride (0.3 g, 2.0 mmol) in dry tetrahydrofuran (60 mL). The reddish black solution was refluxed overnight, cooled, and filtered to remove cobalt metal, CsCl, and LiCl. After removal of the solvent in vacuo, the residue was extracted with hot water (50 mL), the resulting aqueous solution was filtered, and the orange filtrate was treated with triphenylmethylphosphonium bromide (0.56 g, 1.6 mmol). The crude solid formed was extracted with methylene chloride and chromatographed (SiO_2) with 70:30 ethyl acetate/hexane without separation of isomers to afford an orange solid **20** (402 mg, 61% yield), mp 95–97 °C. IR (Nujol, cm^{-1}): 3039 (w), 2911 (s), 2553 (m), 1157 (w), 1116 (w), 1077 (w), 995 (w), 723 (m). ^{11}B NMR (acetone): 5.30 (d, B), 1.18 (d, B), –5.25 (d, B), –6.33 (d, B), –15.63 (d, B), –16.43 (d, B), MS (negative ion FAB): Theoretical ion distribution for $C_{15}H_{35}B_{18}NO_2SCo$ centered around m/e 547.05; observed ion distribution centered around m/e 546. Anal. Calcd for $C_{34}H_{53}B_{18}NO_2SPCo$: C, 49.54; H, 6.48; Co, 7.15. Found: C, 49.20; H, 6.32; Co, 7.00. The diastereomeric products were separated to afford equal amounts of a meso isomer (**20a**) and a *dl* pair of isomers (**20b**) by preparative HPLC on a C_{18} column using a 9:1 acetonitrile/0.1% aqueous trifluoroacetic acid (flow rate 10 mL min^{-1}) solvent mixture.[21]

[7,7′-μ-TosN(CH_2CH_2–)$_2$-(7,8-$C_2B_9H_{10}$)$_2$Fe]$^-$(C_6H_5)$_3$$PCH_3^+$ (21). To a solution of **13** (0.5 g, 0.68 mmol) in dry tetrahydrofuran (70 mL) at 25 °C was slowly added a solution of NaH (0.07 g, 2.7 mmol) dropwise with stirring. The reaction mixture was stirred at reflux temperature for 4 h. When the excess sodium hydride had settled, the clear solution was decanted and then added to a suspension of anhydrous ferric chloride (0.2 g, 1.5 mmol). The resultant red solution was refluxed overnight, cooled, and filtered to remove iron metal, LiCl, and CsCl. After removal of the solvent in vacuo, the residue was extracted with hot water (50 mL), the aqueous solution was filtered, and the red filtrate was treated with triphenylmethylphosphonium bromide (0.5 g, 1.3 mmol) to yield a solid. The crude solid was extracted with methylene chloride and chromatographed (SiO_2) with 80:20 ethyl acetate/hexane without separation of isomers to give a red solid **21** in (329 mg, 59% yield), mp 85–87 °C. IR (Nujol, cm^{-1}): 3039 (w), 2911 (s), 2535 (s), 1157 (m), 1116 (m), 995 (w), 895 (w), 720 (m). ^{11}B NMR (acetone): 100.10, 32.87, 24.53, –0.02, –2.51, –250.0, –525.0. MS (negative ion FAB): Theoretical ion distribution for $C_{15}H_{35}B_{18}NO_2SFe$ centered around m/e 543.96; observed ion distribution centered around m/e 544. Anal. Calcd for $C_{34}H_{53}B_{18}NO_2SPFe$: C, 49.72; H, 6.50; B, 23.69; Fe, 6.80. Found: C, 49.83; H, 6.66; B, 23.50; Fe, 6.67. The diastereomeric products were separated to afford equal amounts of a meso isomer (**21a**) and a *dl* pair of isomers (**21b**) by preparative HPLC on a C_{18} column using a 9:1 acetonitrile/0.1% aqueous trifluoroacetic acid (flow rate 10 mL min^{-1}) solvent mixture.[21]

Collection and Reduction of X-ray Data for 14·CH_2Cl_2. An orange crystal, obtained from a methylene chloride/hexane solution, was mounted on a fiber on a Huber diffractometer constructed by Professor C. E. Strouse of this department. Unit cell parameters were determined from a least-squares fit of 16 accurately centered reflections ($6.4 < 2\theta < 13.3°$). These dimensions and other parameters, including conditions of data collection, are summarized in Table V. Data were collected at 25 °C in the θ–2θ scan mode. Three intense reflections ($2\bar{1}\bar{1}$, $01\bar{3}$, 202) were monitored every 97 reflections to check stability. Intensities of these reflections did not decay and fluctuated less than ±1.0% during the course of the experiment (69.2 h). Of the 4907 unique reflections measured, 1639 were considered observed ($F^2 > 3\sigma(F^2)$) and were used in the subsequent structure analysis. Data were corrected for Lorentz and polarization effects and for secondary extinction. Programs used in this work include locally modified versions of crystallographic programs listed in ref 22.

Solution and Refinement of the Structure 14. Atoms were located by use of direct methods. All calculations were performed on the VAX 3100 computer in the J.D. McCullough Crystallography Laboratory. In

(21) Beckman Research Institute of the City of Hope, Duarte, CA 91010.
(22) CARESS (Broach, Coppens, Becker, Blessing), peak profile analysis, Lorentz and polarization corrections; ORFLS (Busing, Martin, Levy), structure factor calculation and full-matrix least-squares refinement; ORTEP (Johnson) figure plotting; SHELX76 (Sheldrick), crystal structure package; SHELX86 (Sheldrick), crystal structure solution package.

Table V. Details of the Crystallographic Data Collection

	14[a]	15[a]	16[b]	17b[b]
cryst size/mm	0.1 × 0.15 × 0.35	0.10 × 0.15 × 0.25	0.31 × 0.29 × 0.35	0.27 × 0.28 × 0.36
normal to faces	100, 001, 112	010, 001, 100	100, 001, 111	010, 001, 111
appearance	orange platelet	orange platelet	red parallelepiped	yellow parallelepiped
space group	$C2/c$	$P\bar{1}$	$P\bar{1}$	$B2cb$
a/Å	21.726 (5)	10.056 (8)	9.9790 (8)	9.6160 (4)
b/Å	9.906 (2)	11.861 (9)	11.769 (1)	10.7677 (4)
c/Å	35.767 (9)	17.896 (11)	17.640 (1)	18.3258 (7)
α/deg		96.20 (2)	84.458 (2)	
β/deg	103.040 (9)	96.36 (3)	83.610 (2)	
γ/deg		111.20 (3)	112.790 (2)	
V/Å^3	7499	1952	1876	1897
Z	8	2	2	4
ρ(calcd)/g cm^{-3}	1.21	1.19	1.30	1.32
μ/cm^{-1}	5.9 (not applied)	5.7 (not applied)	4.7 (not applied)	10.2 (not applied)
R, R_w, GOF	0.090, 0.107, 2.51	0.089, 0.107, 2.28	0.054, 0.072, 2.28	0.027, 0.038, 1.60

[a] Conditions: temp/K, 298; radiation (graphite monochromator), Mo Kα; wavelength, 0.7107 Å. [b] Conditions: temp/K, 128; radiation (graphite monochromator), Mo Kα; wavelength, 0.7107 Å. GOF = $[\sum w(|F_o| - |F_c|)^2/(N_o - N_v)]^{1/2}$, where $w = 1/(\sigma^2|F_o|)$. $R = \sum||F_o| - |F_c||/|F_o|$. $R_w = [\sum w(|F_o| - |F_c|)^2/\sum w|F_o|^2]^{1/2}$.

Table VI. Positional and Equivalent Isotropic Thermal Parameters for **14**

atom[b]	x	y	z	$\langle u^2\rangle$[a]
Co(3)	0.81392 (12)	0.2397 (3)	0.36968 (7)	0.0473
CB(01)	0.8699 (11)	0.397 (2)	0.3978 (7)	0.072 (7)*
C(02)	0.7998 (9)	0.448 (2)	0.3748 (6)	0.063 (6)*
B(04)	0.8640 (12)	0.261 (3)	0.4267 (7)	0.082 (8)*
B(05)	0.8802 (13)	0.433 (3)	0.4450 (8)	0.092 (10)*
B(06)	0.8383 (13)	0.543 (3)	0.4122 (8)	0.092 (10)*
CB(07)	0.7436 (10)	0.345 (2)	0.3889 (6)	0.077 (7)*
B(08)	0.7780 (12)	0.224 (3)	0.4221 (8)	0.091 (10)*
B(09)	0.8193 (13)	0.325 (3)	0.4623 (8)	0.091 (10)*
B(10)	0.8077 (11)	0.506 (3)	0.4522 (7)	0.065 (8)*
B(11)	0.7579 (13)	0.510 (3)	0.4082 (8)	0.078 (9)*
B(12)	0.7471 (13)	0.378 (3)	0.4362 (8)	0.089 (10)*
C(01′)	0.8380 (9)	0.228 (2)	0.3171 (5)	0.065 (6)*
CB(02′)	0.8855 (10)	0.136 (2)	0.3506 (7)	0.077 (8)*
CB(04′)	0.7640 (9)	0.198 (2)	0.3140 (5)	0.047 (6)*
B(05′)	0.7975 (12)	0.130 (3)	0.2790 (7)	0.074 (8)*
B(06′)	0.8733 (14)	0.095 (3)	0.3021 (8)	0.091 (10)*
B(07′)	0.8352 (12)	0.026 (3)	0.3739 (7)	0.075 (9)*
B(08′)	0.7545 (11)	0.078 (2)	0.3464 (7)	0.058 (7)*
B(09′)	0.7465 (11)	0.038 (3)	0.2974 (7)	0.064 (8)*
B(10′)	0.8174 (13)	−0.035 (3)	0.2920 (8)	0.082 (9)*
B(11′)	0.8729 (13)	−0.032 (3)	0.3366 (8)	0.083 (9)*
B(12′)	0.7918 (14)	−0.070 (3)	0.3351 (8)	0.086 (9)*
C(1M)	0.7879 (11)	0.517 (2)	0.3342 (7)	0.097 (8)*
C(2M)	0.8351 (13)	0.492 (3)	0.3122 (8)	0.137 (11)*
C(3M)	0.8612 (13)	0.359 (3)	0.3020 (8)	0.135 (11)*

[a] Units of isotropic $\langle u^2\rangle$ are Å^2. Units of each esd, in parentheses, are those of the least significant digit of the corresponding parameter. Isotropic values are $[1/(8\pi^2)]$ times the "equivalent B value" defined by Hamilton.[25] An asterisk denotes an atom refined isotropically. [b] Atoms C(08), B(08), B(11), C(11), C(7′), B(7′), B(9′), and C(9′) are included with occupancy of $^1/_2$. See text.

each $C_2B_9H_{10}$ fragment the two atoms adjacent to the bridge-connected carbon have been treated as boron and carbon, each with half-occupancy. These atoms are the following pairs: C(01), B(01); C(07), B(07); C(2′), B(2′); C(4′), B(4′). A solvent molecule, CH_2Cl_2, is located on a 2-fold axis and is disordered. All cation H atoms were included in calculated positions as members of rigid groups: C–H = 1.0 Å, H–C–H = 109.5°, phenyl C_6H_5 with C–C = 1.395 Å. All carboranyl H atoms were kept in located positions. H atoms were assigned u values based approximately on the u value of the attached atom. Scattering factors for H were obtained from Stewart et al.[23] and for other atoms were taken from ref 24. Anomalous dispersion terms were applied to the scattering of Co and P. The maximum and minimum peaks on a final difference electron density map were 0.4 e Å^{-3}. Final positional and thermal parameters for non-hydrogen atoms are given in Table VI.

Table VII. Positional and Equivalent Isotropic Thermal Parameters for **15**

atom	x	y	z	$\langle u^2\rangle$[a]
Co(3)	0.0048 (3)	0.1471 (3)	0.24017 (16)	0.0339
C(1M)	0.222 (2)	0.0413 (18)	0.1748 (11)	0.048 (6)*
C(2M)	0.295 (2)	0.1360 (19)	0.1243 (11)	0.053 (7)*
C(3M)	0.195 (2)	0.1723 (19)	0.0674 (11)	0.051 (7)*
C(4M)	0.130 (2)	0.2600 (17)	0.1006 (11)	0.043 (6)*
C(1)	−0.013 (2)	0.2102 (17)	0.1348 (10)	0.034 (6)*
C(2)	−0.106 (2)	0.058 (19)	0.1310 (12)	0.050 (7)*
B(4)	−0.053 (3)	0.286 (2)	0.2056 (14)	0.043 (8)*
B(5)	−0.130 (3)	0.276 (3)	0.1089 (15)	0.060 (9)*
B(6)	−0.162 (3)	0.136 (2)	0.0621 (14)	0.051 (8)*
B(7)	−0.217 (3)	0.027 (2)	0.2008 (14)	0.045 (8)*
B(8)	−0.188 (3)	0.181 (2)	0.2494 (15)	0.056 (9)*
B(9)	−0.244 (3)	0.260 (3)	0.1816 (15)	0.060 (9)*
B(10)	−0.302 (3)	0.160 (2)	0.0927 (15)	0.058 (9)*
B(11)	−0.291 (3)	0.019 (2)	0.1045 (14)	0.041 (8)*
B(12)	−0.338 (3)	0.101 (2)	0.1803 (14)	0.051 (8)*
C(1′)	0.184 (2)	0.097 (2)	0.2502 (11)	0.036 (6)*
C(2′)	0.225 (2)	0.238 (2)	0.2821 (12)	0.055 (7)*
B(4′)	0.051 (2)	0.009 (2)	0.2909 (12)	0.026 (6)*
B(5′)	0.223 (3)	0.017 (2)	0.3235 (14)	0.047 (8)*
B(6′)	0.342 (3)	0.171 (2)	0.3201 (14)	0.050 (8)*
B(7′)	0.106 (3)	0.255 (2)	0.3473 (14)	0.052 (8)*
B(8′)	−0.009 (3)	0.097 (2)	0.3514 (14)	0.046 (8)*
B(9′)	0.100 (3)	0.020 (2)	0.3874 (14)	0.050 (8)*
B(10′)	0.283 (3)	0.127 (2)	0.4086 (15)	0.056 (9)*
B(11′)	0.288 (3)	0.264 (3)	0.3811 (15)	0.059 (9)*
B(12′)	0.142 (3)	0.176 (2)	0.4227 (15)	0.054 (8)*

[a] See footnote *a* of Table VI.

Collection and Reduction of X-ray Data for 15. An orange crystal, obtained from a methylene chloride/hexane solution, was mounted on a fiber on a Huber diffractometer constructed by Professor C. E. Strouse of this department. Unit cell parameters were determined from a least-squares fit of 16 accurately centered reflections ($6.4 < 2\theta < 13.3°$). These dimensions and other parameters, including conditions of data collection, are summarized in Table V. Data were collected at 25 °C in the θ–2θ scan mode. Three intense reflections (021, 01$\bar{5}$, 202) were monitored every 97 reflections to check stability. Intensities of these reflections did not decay and fluctuated less than ±1.0% during the course of the experiment (72.2 h). Of the 3913 unique reflections measured, 1582 were considered observed ($F^2 > 3\sigma(F^2)$) and were used in the subsequent structure analysis. Data were corrected for Lorentz and polarization effects and for secondary extinction. Other conditions for collection and reduction were the same as those that were applied to **14**.

Solution and Refinement of the Structure 15. Atoms were located by use of heavy-atom methods. All calculations were performed on the VAX 3100 computer. All cation H atoms were included in calculated positions as members of rigid groups: C–H = 1.0 Å, H–C–H = 109.5°.

(23) Stewart, R. F.; Davidson, E. R.; Simpson, W. T. *J. Chem. Phys.* **1965**, *42*, 3175.
(24) *International Tables for X-Ray Crystallography*; Kynoch Press: Birmingham, England, 1974; Vol. IV.
(25) Hamilton, W. C. *Acta Crystallogr.* **1959**, *12*, 609.

Table VIII. Positional and Equivalent Isotropic Thermal Parameters for **16**

atom	x	y	z	$\langle u^2 \rangle^{a,b}$
Fe(3)	0.49918 (6)	0.14447 (5)	0.25865 (3)	0.0155
C(01)	0.6831 (4)	0.0932 (4)	0.2474 (2)	0.0177
C(02)	0.5436 (5)	0.0064 (4)	0.2077 (2)	0.0264
B(04)	0.7274 (5)	0.2423 (4)	0.2150 (2)	0.0168
B(05)	0.8404 (5)	0.1699 (4)	0.1795 (3)	0.0211
B(06)	0.7199 (5)	0.0172 (4)	0.1745 (3)	0.0203
B(07)	0.4925 (5)	0.1000 (5)	0.1451 (3)	0.0211
B(08)	0.6141 (5)	0.2566 (4)	0.1496 (3)	0.0221
B(09)	0.7976 (5)	0.2717 (4)	0.1166 (3)	0.0231
B(10)	0.7899 (5)	0.1282 (5)	0.0901 (3)	0.0242
B(11)	0.6035 (5)	0.0224 (5)	0.1083 (3)	0.0227
B(12)	0.6497 (5)	0.1804 (5)	0.0721 (3)	0.0249
C(1′)	0.3838 (4)	0.0520 (4)	0.3696 (2)	0.0264
C(2′)	0.4777 (4)	0.2020 (4)	0.3685 (2)	0.0219
B(4′)	0.2728 (5)	0.0266 (4)	0.2995 (3)	0.0204
B(5′)	0.1969 (5)	0.0140 (5)	0.3978 (3)	0.0236
B(6′)	0.3289 (5)	0.1247 (5)	0.4414 (3)	0.0239
B(7′)	0.4358 (5)	0.2810 (4)	0.2997 (3)	0.0208
B(8′)	0.3044 (5)	0.1779 (5)	0.2520 (3)	0.0236
B(9′)	0.1472 (5)	0.0956 (5)	0.3247 (3)	0.0231
B(10′)	0.1807 (5)	0.1551 (5)	0.4127 (3)	0.0258
B(11′)	0.3598 (5)	0.2729 (5)	0.3954 (3)	0.0260
B(12′)	0.2494 (6)	0.2566 (5)	0.3234 (3)	0.0269
C(1M)	0.7149 (4)	0.0412 (4)	0.3236 (2)	0.0228
C(2M)	0.7882 (4)	0.1352 (4)	0.3766 (2)	0.0269
C(3M)	0.6881 (5)	0.1705 (4)	0.4333 (2)	0.0278
C(4M)	0.6226 (4)	0.2601 (4)	0.4010 (2)	0.0265

[a] See footnote *a* of Table VI. [b] All tabulated atoms were refined anisotropically.

Table IX. Positional and Equivalent Isotropic Thermal Parameters for **17b**

atom	x	y	z	$\langle u^2 \rangle^{a,b}$
Ni(03)	0.00000	0.00000	0.00000	0.0126
C(01)	0.0865 (6)	0.1116 (4)	–0.0813 (2)	0.0170
C(02)	0.1331 (5)	–0.0351 (5)	–0.0925 (2)	0.0172
B(04)	–0.0948 (7)	0.1275 (5)	–0.0682 (3)	0.0211
B(05)	–0.0119 (7)	0.1630 (4)	–0.1538 (2)	0.0206
B(06)	0.1319 (7)	0.0640 (5)	–0.1680 (3)	0.0204
B(07)	–0.0084 (8)	–0.1280 (4)	–0.0872 (2)	0.0212
B(08)	–0.1622 (6)	–0.0324 (6)	–0.0747 (3)	0.0240
B(09)	–0.1656 (7)	0.0711 (6)	–0.1512 (3)	0.0270
B(10)	–0.0307 (6)	0.0332 (4)	–0.2123 (2)	0.0247
B(11)	0.0667 (7)	–0.0905 (6)	–0.1731 (3)	0.0217
B(12)	–0.1167 (7)	–0.0875 (6)	–0.1626 (3)	0.0263
C(1M)	0.2758 (5)	–0.0882 (4)	–0.0753 (2)	0.0179
C(2M)	0.3880 (5)	–0.0061 (4)	–0.0418 (2)	0.0220

[a] See footnote *a* of Table VI. [b] All tabulated atoms were refined anisotropically.

All carboranyl H atoms were kept in located positions. H atoms were assigned u values based approximately on the u value of the attached atom. Scattering factors for H were obtained from Stewart et al.[23] and for other atoms were taken from ref 24. Anomalous dispersion terms were applied to the scattering of Co and P. Methylene chloride was included (without H) in two unrelated positions with occupancies of 0.3 and 0.2. Constraints were applied to maintain C–Cl = 1.77 Å and Cl–C–Cl = 112°. The maximum and minimum peaks on a final difference electron density map were 0.5 e Å^{-3}. Final positional and thermal parameters for non-hydrogen atoms are given in Table VII.

Collection and Reduction of X-ray Data for 16·$^1/_2$C$_6$H$_{12}$. A red crystal, obtained from a methylene chloride/cyclohexane solution, was mounted on a fiber on a Picker FACS-1 diffractometer modified by Professor C. E. Strouse of this department. Unit cell parameters were determined from a least-squares fit of 50 accurately centered reflections ($10.2 < 2\theta < 20.5°$). These dimensions and other parameters, including conditions of data collection, are summarized in Table V. Data were collected at 128 K in the θ–2θ scan mode. Three intense reflections ($\bar{2}02$, $12\bar{3}$, 015) were monitored every 97 reflections to check stability. Intensities of these reflections did not decay and fluctuated less than ±5.0% during the course of the experiment (120.7 h). Of the 6589 unique reflections measured, 4998 were considered observed ($F^2 > 3\sigma(F^2)$) and were used in the subsequent structure analysis. Data were corrected for Lorentz and polarization effects and for secondary extinction. Other conditions for collection and reduction were the same as those that were applied to **14**.

Solution and Refinement of the Structure 16. Atoms were located by use of heavy-atom methods. All calculations were performed on a VAX 3100 computer. All non-hydrogen atoms were refined with anisotropic parameters. All cation H atoms were included in calculated positions as members of rigid groups: C–H = 1.0 Å, H–C–H = 109.5° (methyl) or angles 120°, C–C = 1.395 Å (phenyl). All carboranyl H atoms were kept in located positions. H atoms were assigned u values = 0.04 Å^2. Scattering factors for H atoms were obtained from Stewart et al.[23] and for other atoms were taken from ref 24. Anomalous dispersion terms were applied to the scattering of Fe and P. Cyclohexane was included with H. The maximum and minimum peaks on a final difference electron density map were 1.0 e Å^{-3}. Final positional and thermal parameters for non-hydrogen atoms are given in Table VIII.

Collection and Reduction of X-ray Data for 17b. A yellow crystal, obtained from a methylene chloride/cyclohexane solution, was mounted on a fiber on a Picker FACS-1 diffractometer modified by Professor C. E. Strouse of this department. Unit cell parameters were determined from a least-squares fit of 87 accurately centered reflections ($7.5 < 2\theta < 20.7°$). These dimensions and other parameters, including conditions of data collection, are summarized in Table V. Data were collected at 128 K in the θ–2θ scan mode. Three intense reflections ($3\bar{1}3$, $04\bar{4}$, $1\bar{3}5$) were monitored every 97 reflections to check stability. Intensities of these reflections did not decay during the course of the experiment (18.8 h). Of the 892 unique reflections measured, 795 were considered observed ($F^2 > 3\sigma(F^2)$) and were used in the subsequent structure analysis. Data were corrected for Lorentz and polarization effects and for secondary extinction. Other conditions for collection and reduction were the same as those that were applied to **14**.

Solution and Refinement of the Structure 17b. Atoms were located by use of heavy-atom methods. All calculations were performed on the VAX 3100 computer. All non-hydrogen atoms were refined with anisotropic parameters. All methylene H atoms were included in calculated positions: C–H = 1.0 Å, H–C–H = 109.5°. All carboranyl H atoms were kept in located positions. H atoms were assigned u values = 0.03 Å^2. Scattering factors for H atoms were obtained from Stewart et al.[23] and for other atoms were taken from ref 24. Anomalous dispersion terms were applied to the scattering of Ni and P. The maximum and minimum peaks on a final difference electron density map were 0.15 e Å^{-3}. Final positional and thermal parameters for non-hydrogen atoms are given in Table IX.

Acknowledgment. We thank the National Institutes of Health for support of this research under Grant CA43904 and for an NIH MARC Predoctoral Fellowship (Grant GM11586) for F.A.G. We also thank the National Science Foundation for a Postdoctoral Fellowship (Grant NSF-CHE 90-01819) for S.E.J. We also thank Albert Calleros for the illustrations.

Supplementary Material Available: Tables of crystallographic details, positional and thermal parameters, and complete interatomic distances and angles (25 pages). Ordering information is given on any current masthead page.